Colloids and Surfaces A: Physicochemical and Engineering Aspects 634 (2022) 128011

Contents lists available at ScienceDirect

Colloids and Surfaces A: Physicochemical and Engineering Aspects

journal homepage: www.elsevier.com/locate/colsurfa

Synthesis of core-brush fluorescent silica nanoparticles with tunable hydrophilicity by ATRP method

M.L. Vera [a,*], J.M. Giussi [b], A. Canneva [b], O. Azzaroni [c], A. Calvo [b]

[a] Centro de Investigación y Desarrollo en Materiales Avanzados y Almacenamiento de Energía de Jujuy (CIDMEJU). Universidad Nacional de Jujuy-CONICET, Av. Juan A.Rojas, Palpalá, Jujuy, Argentina
[b] YPF Tecnología (Y-TEC), La Plata, Bs. As., Argentina
[c] Instituto de Investigaciones Fisicoquímicas Teóricas y Aplicadas (INIFTA), Universidad Nacional de La Plata –CONICET, La Plata, Argentina

HIGHLIGHTS

- A zwitterionic polymer shell was successfully grafting from a fluorescent silica core via ATRP method.
- The ratio between the activation-deactivating species, Cu(II)/Cu(I), determines the conformational regime of the polymer chains and the graft density.
- Nanoparticles with tunable colloidal stability in brine and non-polar media were obtained.

GRAPHICAL ABSTRACT

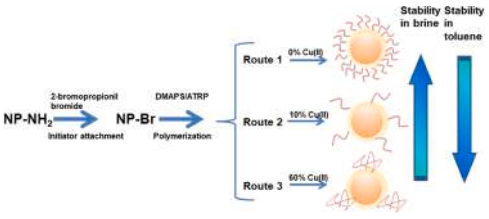

ARTICLE INFO

Keywords:
Core-brush fluorescent silica nanoparticles
Tailor made functional hybrid nanoparticles
Hydrophobic/hydrophilic nanocomposite
DMAPS-functionalized colloids
ATRP polymerization

ABSTRACT

Polymer coating on fluorescent silica nanoparticles enables to tailor made nanocomposite with unique tunable properties. Combining the emission of a fluorescent probe and the surface chemistry of a polymer shell a wide range of applications can be cover. The changing in the conformation of polymer chains enables to modify the hydrophilicity of the functionalized particles. For this, zwitterionic polymers are optimal since the electrostatic interaction between charged groups determines the conformational regime of the chains and the colloidal stability of the particle. In this work, we propose a functionalization of Amino Fluorescent Silica Nanoparticles (Amino-NPF) with a zwitterionic polymer by ATRP method. Poly [2- (Methacryloyloxy) ethyl] dimethyl- (3-sulfopropyl) ammonium hydroxide (PDMAPS) was successfully grafted onto the Amino-NPF surface. In particular, we followed three routes with different amount of catalyst. Route 1 corresponds to non-Cu (II) in solution, while pathways 2 and 3 consist of an increment in the metal concentration, 10% and 60% relative to Cu (I), respectively. A very short reaction time, only 15 min, was employed to diminish or avoid radical-radical termination. The stability and dispersability of the obtained core-brush nanoparticles in different solvents was evaluated. We demonstrate that the Cu (II) to Cu (I) concentration ratio defines the conformation of the polymer chains and in turn the hydrophilic character of the particles.

1. Introduction

Hybrid systems as organic-inorganic nanoparticles are smart components for a wide range of applications ranging from nanomedicine to oil and gas exploration [1,2]. Mechanical and thermal properties of hybrid nanocomposites [3] can be tailor-made depending

* Corresponding author.
E-mail address: mlvera@cidmeju.unju.edu.ar (M.L. Vera).

https://doi.org/10.1016/j.colsurfa.2021.128011
Received 8 October 2021; Received in revised form 23 November 2021; Accepted 25 November 2021
Available online 29 November 2021

on the requirements of their application, enhancing the compatibility between the matrix and nanoparticles [4,5].

These systems are highly interesting structures since they combine synergistically the advantageous physical-chemical properties of both inorganic core and polymeric shell, providing superior functionality to the final material. The correct design of the surrounding organic layer will get an enhanced compatibility between hybrid nanomaterial and the surrounding medium. In this context, it is possible to tailor-made the nanocomposite depending on the final application [3,6–8]. Core-brush fluorescent nanoparticles with covalently linked polymer chains have attracted increasing interest due to their facile synthesis, detection, stability and tunable dispersibility [9–11]. Several works have been reported to show that it is possible to control the stability, mechanical and physical properties of nanocomposites with the control of the surface chemistry by an adequate functionalization [12–15].

Although it is possible to design nanocomposites with a wide range of inorganic oxides, silica nanoparticles have received much attention considered their unique properties including facile synthesis and functionalization, tailorable structure, high surface areas, good physicochemical stability, cost effective production and favorable biocompatibility [16–19]. Functionalization of the silica surface can be carried out physically (by physisorption) or chemically (through covalent bonding). The first one is not a favored technique because the non-covalent character makes the absorption reversible especially during processing. In the other hand, covalent grafting is preferred to maximize a stable interfacial compatibility between the inorganic core and polymer shell. Chemical techniques involves either "grafting to'' or "grafting from'' methods. By "grafting to'' approach preformed reactive macromolecules with compatible surface groups, reacts with the inorganic substrate. It is an experimentally simply method but has some limitations, the most relevant is the low grafting density because of steric crowding of reactive sites by previously attached polymers [20]. Through "grafting from'' method, also called Surface Initiated Polymerization (SIP), the grafting density is higher because the access of small monomer molecules to the active initiation sites are not sterically limited. This technique is a powerful alternative to control the functionality, density and thickness of polymer brushes with almost molecular precision [21]. The SIP method can be carried out following either conventional free or controlled radical polymerization. Some advantages from non-controlled radical polymerization involve simple equipment, low cost process and facile to scale up [22,23]. However, controlled radical polymerization allows a better control of the polydispersion and molecular weight of grafted polymer chains, generating polymers with well-defined architectures [24].

In general, controlled/living polymerization can be achieved by stable free radical polymerization, e.g Atom Transfer Radical Polymerization (ATRP) [25,26]. This method implies the surface modification of silica nanoparticle (NP) with an initiator that provides the radical point for polymer growth. It is a metal catalyzed process where metal-ligand species play the role of activating-deactivating the growing polymer chain. A wide variety of ATRP initiators and monomers with different couples of metal-ligand species can be used. C. Huang et al., studied the polymerization of methyl methacrylate on silica NP and the effect caused by the initiator spacer length on grafting density using both CuCl and CuBr as catalysts [27]. Lilin Zhou et al., have synthetized Poly ((2-Dimethylamino)ethyl methacrylate) (PDMAEMA) on silica nanoparticles surface to form pH and temperature responsive hybrid NP [28]. In particular, zwitterionic polymers have attached attention because of their unique quality of anti-biofouling, replacing the traditional polyhydrophilic films such as PEG [22]. So it is possible to tailor-made a core-brush type nanoparticle according to a specific requirement of the application media.

In this work, we propose the synthesis of an inorganic-organic nanocomposite with tunable hydrophilicity by a fast ATRP. For this, the polymerization of Poly [2-(Methacryloyloxy)ethyl]dimethyl-(3-sulfopropyl)ammonium hydroxide (PDMAPS) was done via three routes of synthesis, 1, 2 and 3, where the amount of Cu(II) to Cu(I) was modified. The reaction time was 15 min as a strategy to avoid radical-radical terminations. The obtained results demonstrated that it is possible to synthesize particles with extremely different hydrophilicity by varying the ATRP catalyst concentration.

2. Materials and methods

2.1. Materials

2- bromopropionyl bromide (Br-isobutirate) 97%, triethylamine, [2-(Methacryloyloxy)ethyl]dimethyl-(3-sulfopropyl)ammonium hydroxide (DMAPS), 2,2´-bipyridine (99%, bipy), copper I chloride (99.9% CuCl), copper II chloride (97%, CuCl2) and. Tetrahydrofuran (THF) were purchased from Sigma-Aldrich. Tetrahydrofuran (THF) All chemicals were used as received. Water used was deionized (18 MΩ cm) Absolute ethanol and methanol were obtained from Merck.Amino fluorescent silica nanoparticles (Amino-NPF) were synthetized following our previous report [29].

2.2. Immobilization of ATRP initiator (Br-isobutirate) on Amino-NPF surface

This stage of synthesis was common to the three routes, 1, 2 and 3. The dry Amino-NPF were redispersed in anhydrous THF in a three-neck flask after 20 min sonication (0.5% m/v). To avoid heating the sample, ice was employed in the sonication bath. Then, the flask was introduced in a water bath with ice and mechanical stirring was set up at 800 rpm. Triethylamine and Br-isobutirate were added sequentially (0.64 and 0.50 ml, respectively). Previous to the addition of the initiator, the system was bubbled with N_2 for a few minutes. After 10 min, the ice was removed and the heating plate was set up to 25 °C. The reaction was carried out overnight. Previous to evaporate the solvent, distilled water was added to the reaction mixture to liberate possible vapors of HBr, under extractor. A rotary evaporator was employed to eliminate the THF. Then the mixture was diluted with distilled water and four cycles centrifugation/ change of solvent/ sonication were complete. The first wash was done with absolute ethanol; in the others one a mixture of methanol and water (4:1 in volume) was used. NP-Br were storage in 20 ml of water:methanol mixture in refrigerator until used.

2.3. Synthesis of PDMAPS NP

This step was developed following three pathways, although the experimental protocol was the same for all of them, different Cu(II) concentrations were employed for each one. Route 1 corresponds to Non-Cu(II), route 2 to a 10% (0.0495 g, $CuCl_2$) and route 3 to a 60% (0.0297 g, $CuCl_2$). In a schlenk tube, 10 ml of the suspension of NP-Br previously obtained was bubbled with N_2 for 30 min and mixed with 0.1575 g of bipy and the quantity of Cu(II) corresponding to each route of synthesis. Then, the system was bubbled with N_2 for 10 more minutes and 0.0495 g of Cu(I) were added. N_2 was bubbled for 10 more minutes. While, in another schlenk tube 1.4 g of DMAPS was dissolved in 10 ml of the methanol:water mixture and bubbled with N_2 for 40 min. Then this suspension was added to the reaction mixture under stirring (800 rpm) and an atmosphere of N_2. The reaction was carried out for 15 min. To ensure the end of the polymerization, the system was exposed to oxygen and distilled water was added. Immediately the solution color changed from brown to blue, indicating that the Cu-bipy complex was destroyed. Finally, four wash cycles were complete with warm water following the sequence of centrifugation/ change of solvent/ sonication.

2.4. Equipment and characterization

2.4.1. Dinamic Light Scattering (DLS)

DLS measurement was performed in a BI-200SM Goniometer Ver.2.0

Table 1
hydrodynamic diameter, D_h (nm), in water and brine obtained by DLS from NPs without functionalization and functionalized NPs at a concentration of 0.01 mg/ml.Nacional de Investigaciones Científicas y Técnicas

Sample	$D_{h\ (water)}$	$D_{h\ (brine)}$
Amino-NPF	210	Not stable
NP-1	390	540
NP-2	750	1000
NP-3	Not stable	Not stable

(Brookhaven Instrument Corp.) scanning the range of 30–150° every 10° (λ = 637 nm). Samples were prepared in water at a concentration of 0.01 mg/ml and measured in a DLS plastic vial. Hydrodynamic diameter (D_h) of the particles was calculated using the Stokes-Einstein equation from the cumulant analysis from Brookhaven Instruments built-in software package.

2.4.2. X-ray photoelectron spectroscopy (XPS)

XPS analysis was done with a SPECS instrument located at Y-TEC Company. Spectra were acquired using a monochromatic AlKα (1486.6 eV), a spectrometer equipped with a dual anode Al/Ag X-ray source and a hemispherical electron energy analyzer. Binding energies are referred to the adventitious C 1 s emission at 285 eV. Measurements were performed on dry powdered samples using a conducting double stick carbon tape.

2.4.3. Fluorescence Emission

Room temperature luminescence measurements were performed with a Jobin-Yvon Spex Fluorolog FL3–11 Spectrometer at INIFTA, which is equipped with a Xe lamp as the excitation source, a monochromator with 1 nm bandpass gap for selecting the excitation and emission wavelengths, and a red sensitive R928 PM detector. The spectra were corrected for the wavelength-dependent sensitivity of the detector and the source. Furthermore, emission spectra were corrected for Raman scattering by using the solvent emission spectrum. Samples were diluted in water at a concentration of 0.01 mg/ml. Excitation was done at 490 nm and emission was collected between 500 and 640 nm.

3. Results and discussion

The sized-controlled fluorescent silica Nanoparticles with a surface coverage of amino groups (Amino-NPF) were obtained following the one pot synthesis previously reported by us [29]. Briefly, all the reactants were incorporated to the reaction mixture in an established sequence under continuously stirring: ethanol, APTES, FITC, ethanol, TEOS, ammonia and water. Between each addition an interval of one minute was considered. After a reaction time of 24 h, the Amino-NPF were washed with absolute ethanol through three cycles of centrifugation)/sonication/redispersion. Finally, the solvent was evaporated in an oven at 100 °C for one night.

Surface modification of the Amino-NPF was performed by two steps, as was described in Section 2. Firstly, the initiator of the polymerization, Br-isobutirate, was covalently linked to the superficial amino groups in an anhydrous media. After this, type core-brush NPs of fluorescent silica were obtained with brushes of poly(DMAPS), PDMAPS. We evaluated the PDMAPS grafting on NPs via three different routes of polymerization: 1, 2 and 3, were the concentration of Cu(II) was varied. In the first one, non-Cu(II) was employed, while in routes 2 and 3, 10% and 60% of Cu(II) respect to Cu(I) was used.

DLS provides value information relative to the level of aggregation and interaction between particles in solution. Table 1 presents the hydrodynamic diameter (D_h) in water and brine obtained from NP without functionalization (Amino-NPF) and functionalized NPs via the three routes (NP-1, NP-2 and NP-3). The particle concentration was 0.01 mg/ml.Consejo Nacional de Investigaciones Científicas y Técnicas

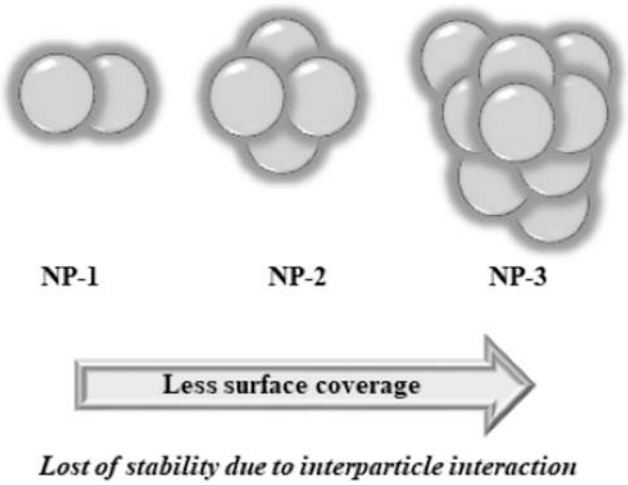

Fig. 1. schematic representation of hydrodynamic behavior of functionalized NP in water or brine media.

It is important to notice that it was not possible to disperse unmodified NPs in brine neither NPs obtained from route 3 in water or brine. Results obtained from the other samples show an increment in the hydrodynamic diameter (D_h) after polymerization. Amino-NPF presents a D_h equal to 210 nm. After polymer grafting on silica surface, the diameter of the particles changes to 390 nm for route 1 (NP-1) and 750 nm for pathway 2 (NP-2). In both cases these values indicate the presence of clustering, probably due to electrostatic interaction between polymer chains of neighboring particles. A medium without electrolytes is not the more appropriate for a zwitterionic polymer. In brine it is expect that polymer chains adopt an extended conformation, exposing charge groups to the surrounding media [30]. Values for hydrodynamic diameter in this condition show a considerable increment respect to the values in water, 390–540 nm for NP-1 and 750–1000 nm for NP-2. Nevertheless, these results indicate interaction between particles that are more relevant in the case of particles polymerized via route 2. For NP-3 it was not possible to determine a hydrodynamic diameter in aqueous media. This result is not definitive to establish the absence of polymer on particles surface. It is possible to obtain an hydrophobic particle if polymer chains adopt a collapse conformation [31].

Additionally NP-1 and NP2 were characterized by SEM; Fig. S1Supporting Information. Still under ultra-vacuum conditions, it can be observed a high degree of agglomeration between particles in the case of NP-2. It is in agreement with the results obtained from DLS that suggested that an increment in the percentage of Cu(II) in the reaction mixture lead to particles with more tendency to clustering. Due to the insolubility in water of NP-3, these particles were not characterized by SEM. To obtain comparable results, in function of the polymer conformation, it is necessary that the samples were dried from the same solvent.

Fig. 1 presents a schematic representation of the possible behavior of functionalized particles in water.

The results obtained from DLS can be easily correlated with visual analysis. Fig. 2 shows the photographs of colloidal suspension of bare NP, NP-Br, NP-1, NP-2 and NP-3 in water, brine and toluene (0.1% w/v).

It is clearly that bare silica NPs (Amino-NPF) are stable in water but not in brine or toluene. These particles were obtained by a one-pot synthesis procedure where TEOS and APTES co-condensate together. As a result, an important percentage of amino groups are exposed on the surface and give colloidal stability to the particles in water but make them insoluble in non-polar media or brine. In the case of NP-Br a poor solubility is observed in water and brine, and a little stability in toluene. Nanoparticles obtained from route 1 and 2 present similar solubility in water, while NP-1 are more soluble in brine but insoluble in toluene. In

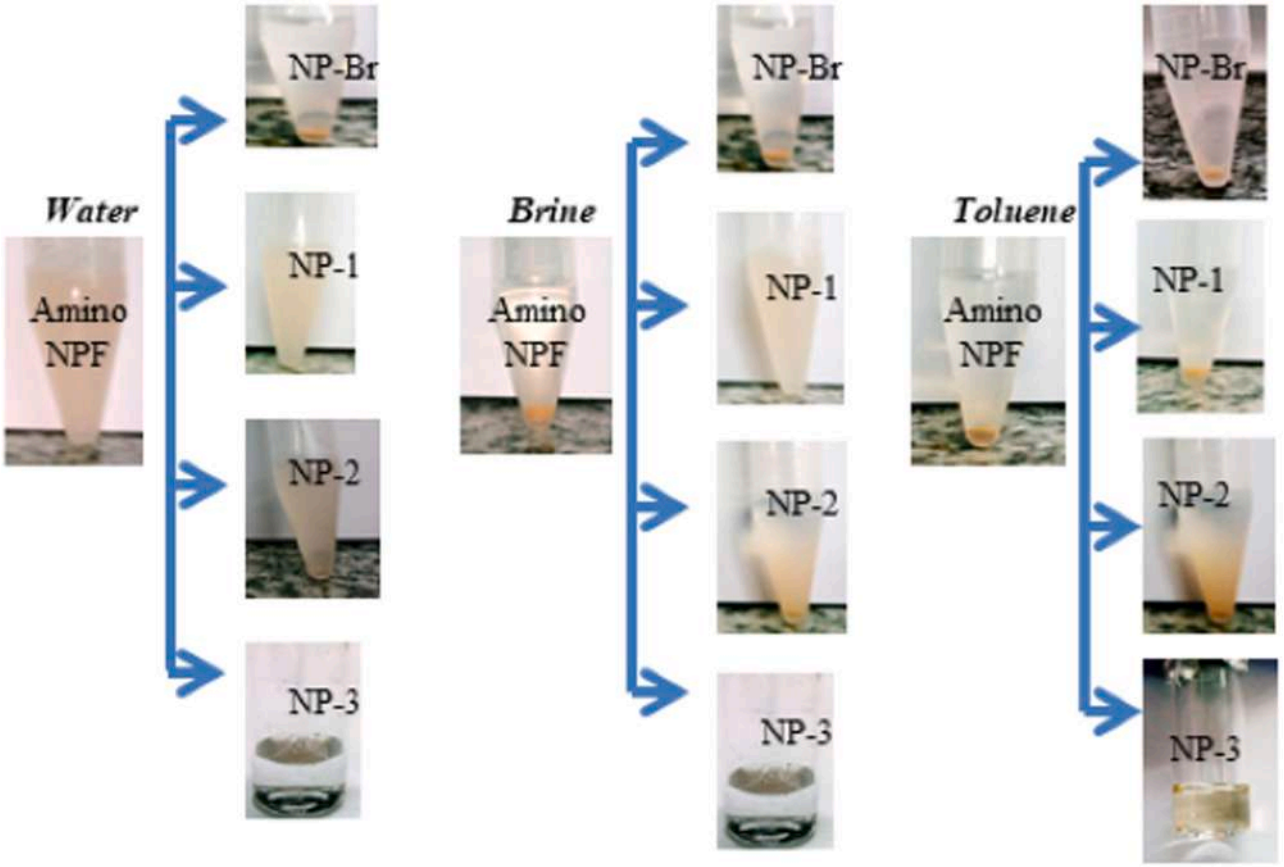

Fig. 2. photographs of dispersions obtained from unmodified silica Amino-NPF, NP-Br and functionalized NP via route 1, 2 and 3 (up to down) in three different solvents: water, brine and toluene (left to right).

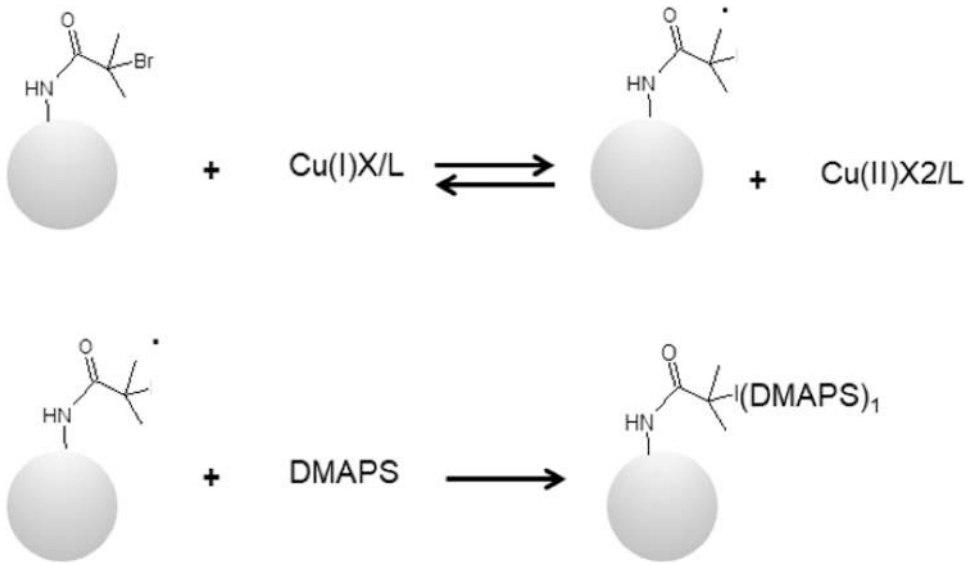

Fig. 3. schema of the initial activation of radical points by the presence of Cu(I)-Cu(II) redox cuple.

the other hand, NP-2 are partially stable in brine and toluene. Finally, NP-3 are insoluble in water and brine, and totally soluble in non-polar solvent. This behavior evidence the presence of polymer chains on this nanoparticles surface. While Amino-NPF and NP-Br are insoluble and partially soluble in toluene, NP-3 are totally soluble in this solvent. So following the route 3 of polymerization it is possible to obtained a hydrophobic particle, while following the other routes, 1 and 2, hydrophilic and partially hydrophilic particles are obtained.

The transition from a hydrophilic regime to a hydrophobic one is strongly dependent of the Cu(II)/Cu(I) relationship in the reaction mixture [32]. Cu(II) has the role of slow down or deactivate the ´living´´ character of the brush growth. Fig. 3 schematizes the initial activation.

It is seen in the schema show in Fig. 3 that the redox activity of copper couple controls the first stage of the polymerization process,

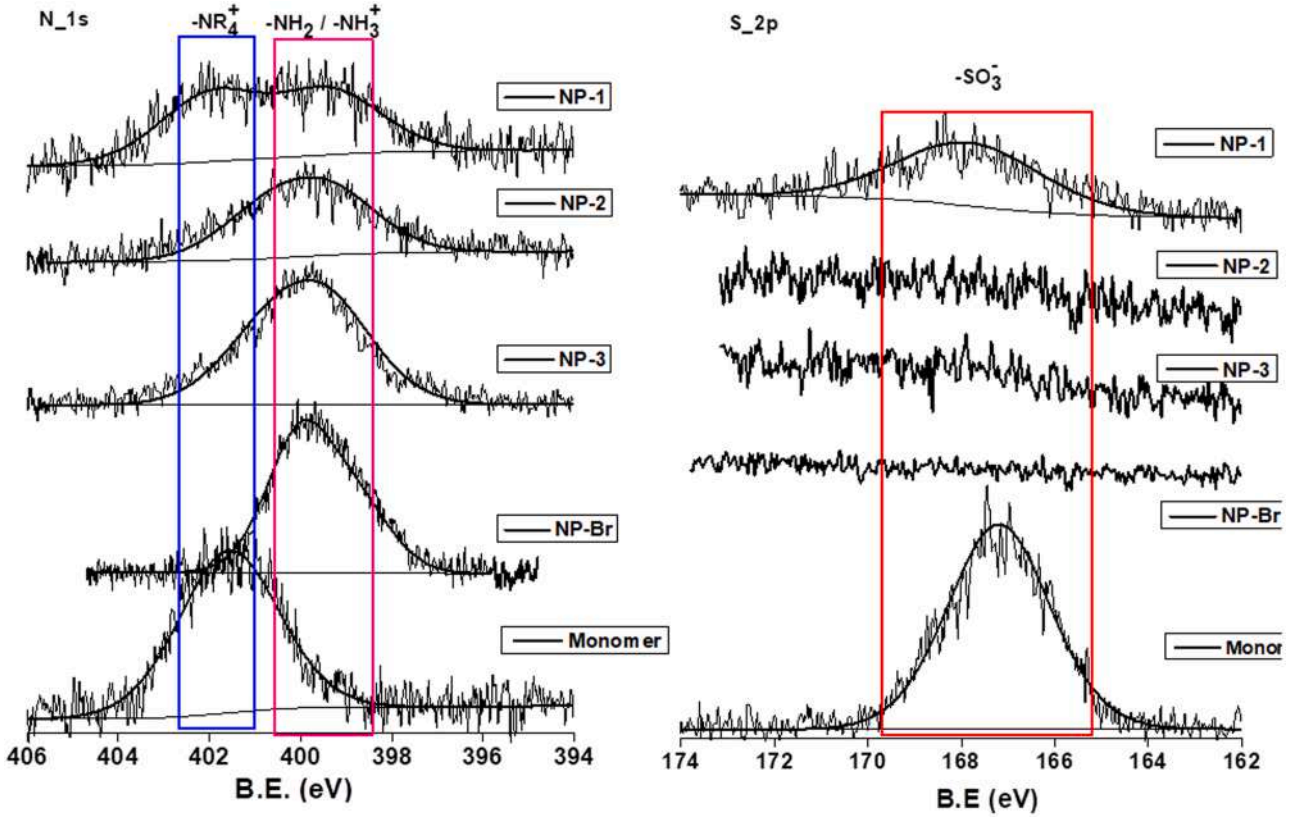

Fig. 4. N_1S and S_2p (left and right) XPS spectra of monomer, NP-Br, NP-3, NP-2 and NP-1 (bottom to up).

where the halide is transfer to generate a radical point on silica surface.

Through routes 1, 2 and 3 the catalyst is added to the reaction mixture containing modified NP with the halide initiator (NP-Br) and in a final step the monomer is incorporated. Then the reaction takes place for only 15 min, to avoid radical-radical termination. By this pathway of synthesis the activation of initial radicals will depend on the concentration of activating/deactivating copper redox couple. Each radical point on nanoparticles surface is a potential point for anchoring the monomer and in consequence the polymer chain. When Cu(II) is present from the starting mixture, the halide transfer from the NP surface is diminished. Due to this, the result is similar to that obtained in a synthesis carried out with less initiator concentration. A decrease in the initial grafting density implies a poor surface coverage of the particles and due to this, the conformation of the polymer chains change from the so-called "brushes regime" to the so-called "mushroom regime" [33]. In the last one, charge groups are occluded in the inner of the shell and ions from the media cannot diffuse between the chains and colloidal stability is lost. Based on this, it is expected that functionalized NP obtained from route 3 (NP-3), where 60% of Cu(II) was employed, have not stability in water but solubilize in non-polar media. While NP obtained from route 1 (NP-1) where no copper is employed, reached the best colloidal stability in water and brine. Finally, NP obtained from route 2 (NP-2) present an intermediate behavior.

Nanoparticles functionalized with initiator (NP-Br) and those obtained through the three routes of synthesis (NP-1, NP-2 and NP-3) were characterized by XPS. Monomer was used as reference for characteristic signals. Fig. 4 shows N_1S and S_2p spectra.

Looking at N_1s spectrum of the monomer only one signal is observed nearly 402 eV that correspond to the quaternary amine [34]. When analyzing the spectrum of NP-Br is clearly identified the wide signal located in the region of amino/ammonium species on nanoparticles surface. Finally, this signal is displaced to the quaternary amine region as the spectra of the polymerized NP are observed. Np-1 show the most

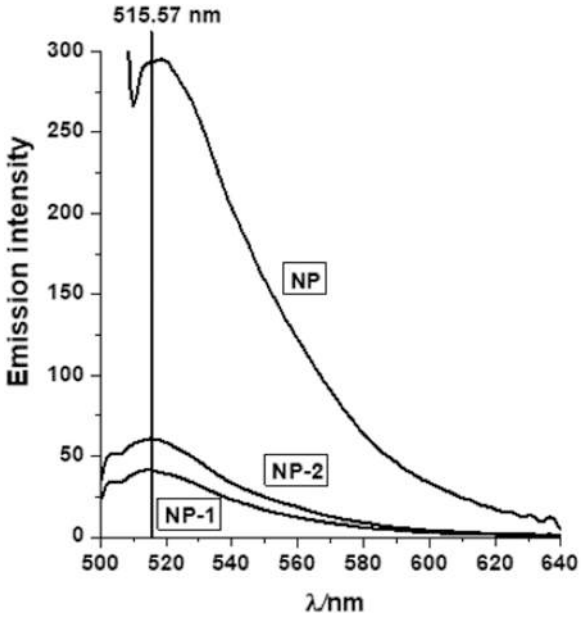

Fig. 5. fluorescence emission spectra obtained from bare NP, NP-1 and NP-2 in water. λ_{exc}= 490 nm.

clearly displacement, while NP-2 and NP-3 show a wider signal. In the case of S_2p spectra, it is expect to find the peak of sulfonate group in the vicinity of 168 eV [35] only if polymer is present in an appropriate conformation and quantity. The absorption cross section of sulfur is similar to the N [36], but this element is absent in the starting particles, so it is necessary to have sufficient emitted electrons to distinguish this signal. In the case of the monomer, it is clear the peak of the sulfonate

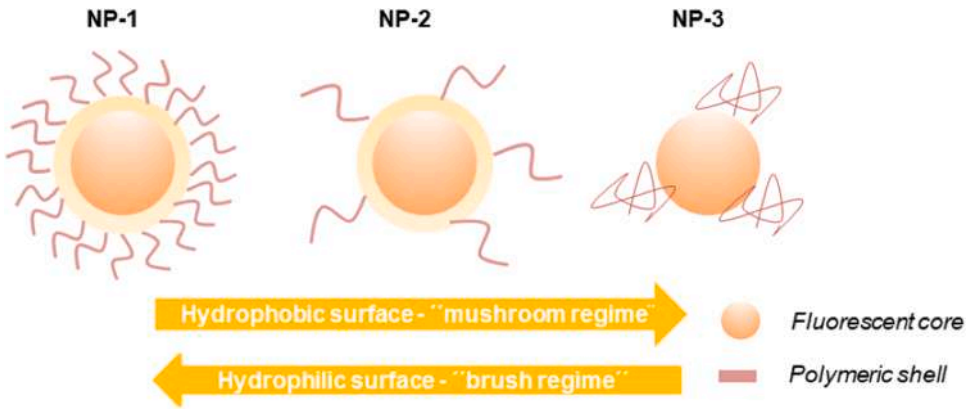

Fig. 6. schematizes the particles that are obtained from each route of synthesis: 1, 2 and 3, and the polymer chain conformation in brine media.

group. In the spectrum of NP-Br the signal is absent because non polymer was grafted on this nanoparticles. Nevertheless, in the case of NP-2 and NP-3, were non signal is observed, it is not possible to conclude the absence of polymer chains. It is necessary to consider the quantity of polymer brushes and the spatial conformation of them (as it was discussed above). Through route 2 and 3 due to the increment in Cu(II) concentration, the graft density was less than on particles obtained from route 1 and polymer chains adopted a more collapsed conformation. These factors may hinder the characteristic signal of sulfonate group.

Finally, fluorescence emission of bare NP, and particles functionalized via route 1 and 2 were measured to evidence not damage of fluorophore during the polymerization. Samples were prepared in water at a concentration of 0.01 mg/ml. Excitation was done at 490 nm and emission collected between 500 and 650 nm. Fig. 5 shows the spectrum obtained from each case.

Fluorescence emission was detect at 515,57 nm in all cases, Fig. 5, that it characteristic of FITC emission in silica matrix [29]. It is evident that the polymerization procedure not alters the core property of the nanoparticles. The difference observed in the intensity of the signal is due to the scattering contribution as a result of interparticle interaction. This effect is less important in particles with surface coverage (NP-1 and NP-2) than bare NP. Fluorescence emission although demonstrate that nanoparticles polymerized from route 1 are more stable than those obtained from route 2.

In summary, we report for the first time a fast grafting-from polymerization method where a variation in the concentration of the deactivating metal Cu(II), enable to synthetized particles with a tunable hydrophlilicity. Results have demonstrated that the catalyst Cu(II)/Cu(I) ratio determines the initial graft density of radical points and the conformation of the polymer chains on silica surface. These qualities have influence in the transition from a brush-regime to a mush-room one.

4. Conclusions

Core-brush NP with tunable hydrophilicity were designed and synthetized by grafting from approach of PDMAPS on fluorescent silica NP surface. The colloidal stability and the dispersability of the functionalized particles were evaluated by a crossed characterization. The obtained results demonstrate that the concentration of Cu(II) has a noticeable effect on the graft density and conformational regime of the polymer. From this way it is possible to control the hydrophilic character of the core-brush particles by selecting the adequate catalyst concentration. We report three pathways for PDMAPS grafting on fluorescent silica nanoparticles, where the concentration of Cu(II) was varied from 0% to 60% relative to Cu(I). When non Cu (II) is used, route 1, a totally hydrophilic particle is obtained, with polymer chains in the brush-regime with high surface coverage and short brushes. This enables colloidal stability in water or brine media. In the other hand a high concentration of Cu(II) (60%), route 3, leads to a totally hydrophobic particle with polymer chains in the mushroom-regime, with a poor surface coverage and a collapsed conformation. Due to this, there is interparticle clustering in polar media. Finally, a low concentration of deactivating (10% of Cu(II)), route 2, enables the synthesis of particles with an intermediated behavior with a moderate graft density.

Fig. 6 schematizes the particles that are obtained from each route of synthesis: 1, 2 and 3, and the polymer chain conformation in brine media.

In this work we obtained core-brush type nanoparticles with a tunable colloidal stability that enables to cover a wide range of applications. NP obtained via route 1, with a high stability in brine media, could exhibit a great potential in nano-medicine as carriers or fluorescent markers with non-fouling effect. Mixed-charge coverage could avoid the adhesion of serum proteins [36]. Functionalized NP synthetized by route 2, with the capability to solubilize in polar and nonpolar media in an adequate concentration, could be potentially employed as partitionable tracers in oil and gas studies. In this case, the equilibrium distribution of the tracers between the brine phase and the oil one provides value information respect to oil saturation [37]. Finally, particles obtained from route 3, with a totally hydrophobic behavior could be employed to study the purity of petroleum derivate as gasoline. E.g., if the polarity of the media is change due to the introduction of a polar additive the solubility of the particles will be decreased and in turn the total fluorescence emission [38].

CRediT authorship contribution statement

M.L. Vera: Conceptualization, Formal analysis, Investigation, Methodology, Writing – original draft, review & editing. **J.M. Giussi:** Conceptualization, Investigation, Methodology, Resources. **A. Canneva:** Investigation, Formal analysis, Writing – review & editing. **O. Azzaroni:** Methodology, Investigation, Methodology, Resources. **A. Calvo:** methodology, Resources, Supervision, Funding acquisition.

Declaration of Competing Interest

The authors declare that they have no known competing financial interests or personal relationships that could have appeared to influence the work reported in this paper.

Acknowledgments

J.M. Giussi, A. Canneva and O. Azzaroni are research members of CONICET, Argentina. This research was supported by the grant PICT 2012–2359 and FONARSEC-Nanotecnología 2012/01 from ANPCyT, and by YFP Tecnología S. A.

Appendix A. Supporting information

Supplementary data associated with this article can be found in the online version at doi:10.1016/j.colsurfa.2021.128011.

References

[1] R. Huang, Y.-W. Shen, Y.-Y. Guan, Y.-X. Jiang, Y. Wu, K. Rahman, L.-J. Zhang, H.-J. Liu, X. Luan, Mesoporous silica nanoparticles: facile surface functionalization and versatile biomedical applications in oncology, Acta Biomater. 116 (2020) 1–15, https://doi.org/10.1016/j.actbio.2020.09.009.

[2] S. Azarshin, J. Moghadasi, Z.A. Aboosadi, Surface functionalization of silica nanoparticles to improve the performance of water flooding in oil wet reservoirs, Energy Explor. Exploit. 35 (6) (2017) 685–697, https://doi.org/10.1177/0144598717716281.

[3] K. Shiba, M. Ogawa, Precise synthesis of well-defined inorganic-organic hybrid particles, Chem. Rec. 18 (7–8) (2018) 950–968, https://doi.org/10.1002/tcr.201700077.

[4] S.R. Karnati, D. Oldham, E.H. Fini, L. Zhang, Surface functionalization of silica nanoparticles to enhance aging resistance of asphalt binder, Constr. Build. Mater. 211 (2019) 1065–1072, https://doi.org/10.1016/j.conbuildmat.2019.03.257.

[5] C.R. Miranda, L.S. de Lara, B.C. Tonetto, Stability and Mobility of Functionalized Silica Nanoparticles for Enhanced Oil Recovery Applications, 2012.

[6] C. Sanchez, G.Jd.A.A. Soler-Illia, F. Ribot, T. Lalot, C.R. Mayer, V. Cabuil, Designed hybrid organic−inorganic nanocomposites from functional nanobuilding blocks, Chem. Mater. 13 (10) (2001) 3061–3083, https://doi.org/10.1021/cm011061e.

[7] S. Bashir, J. Liu, Chapter 1 - nanomaterials and their application, in: J.L. Liu, S. Bashir (Eds.), Advanced Nanomaterials and their Applications in Renewable Energy, Elsevier, Amsterdam, 2015, pp. 1–50.

[8] M.A. Macchione, C. Biglione, M. Strumia, Design, synthesis and architectures of hybrid nanomaterials for therapy and diagnosis applications, Polymers 10 (5) (2018), https://doi.org/10.3390/polym10050527.

[9] L. Huang, S. Yang, J. Chen, J. Tian, Q. Huang, H. Huang, Y. Wen, F. Deng, X. Zhang, Y. Wei, A facile surface modification strategy for fabrication of fluorescent silica nanoparticles with the aggregation-induced emission dye through surface-initiated cationic ring opening polymerization, Mater. Sci. Eng.: C. 94 (2019) 270–278, https://doi.org/10.1016/j.msec.2018.09.042.

[10] J.E. Fuller, G.T. Zugates, L.S. Ferreira, H.S. Ow, N.N. Nguyen, U.B. Wiesner, R. S. Langer, Intracellular delivery of core–shell fluorescent silica nanoparticles, Biomaterials 29 (10) (2008) 1526–1532, https://doi.org/10.1016/j.biomaterials.2007.11.025.

[11] A.M. Santiago, T. Ribeiro, A.S. Rodrigues, B. Ribeiro, R.F.M. Frade, C. Baleizão, J. P.S. Farinha, Multifunctional hybrid silica nanoparticles with a fluorescent core and active targeting shell for fluorescence imaging biodiagnostic applications, Eur. J. Inorg. Chem. 2015 (27) (2015) 4579–4587, https://doi.org/10.1002/ejic.201500580.

[12] Z. Guo, T. Pereira, O. Choi, Y. Wang, H.T. Hahn, Surface functionalized alumina nanoparticle filled polymeric nanocomposites with enhanced mechanical properties, J. Mater. Chem. 16 (27) (2006) 2800–2808, https://doi.org/10.1039/B603020C.

[13] V. Vergnat, T. Roland, G. Pourroy, P. Masson, Effect of covalent grafting on mechanical properties of TiO2/polystyrene composites, Mater. Chem. Phys. 147 (1) (2014) 261–267, https://doi.org/10.1016/j.matchemphys.2014.04.038.

[14] Y.-Y. Yuan, C.-Q. Mao, X.-J. Du, J.-Z. Du, F. Wang, J. Wang, Surface charge switchable nanoparticles based on zwitterionic polymer for enhanced drug delivery to tumor, Adv. Mater. 24 (40) (2012) 5476–5480, https://doi.org/10.1002/adma.201202296.

[15] N.K. Maurya, P. Kushwaha, A. Mandal, Studies on interfacial and rheological properties of water soluble polymer grafted nanoparticle for application in enhanced oil recovery, J. Taiwan Inst. Chem. Eng. 70 (2017) 319–330, https://doi.org/10.1016/j.jtice.2016.10.021.

[16] C. Bharti, U. Nagaich, A.K. Pal, N. Gulati, Mesoporous silica nanoparticles in target drug delivery system: a review, Int J. Pharm. Invest. 5 (3) (2015) 124–133, https://doi.org/10.4103/2230-973x.160844.

[17] N. Tsubokawa, T. Kimoto, K. Koyama, Polymerization of vinyl monomers in the presence of silica having surface functional groups, Colloid Polym. Sci. 271 (10) (1993) 940–946, https://doi.org/10.1007/BF00654853.

[18] R. Kamegawa, M. Naito, K. Miyata, Functionalization of silica nanoparticles for nucleic acid delivery, Nano Res. 11 (10) (2018) 5219–5239, https://doi.org/10.1007/s12274-018-2116-7.

[19] P.G. Jeelani, P. Mulay, R. Venkat, C. Ramalingam, Multifaceted application of silica nanoparticles. A review, Silicon 12 (6) (2020) 1337–1354, https://doi.org/10.1007/s12633-019-00229-y.

[20] C.J. Fristrup, K. Jankova, S. Hvilsted, Surface-initiated atom transfer radical polymerization—a technique to develop biofunctional coatings, Soft Matter 5 (23) (2009) 4623–4634, https://doi.org/10.1039/B821815C.

[21] S. Edmondson, V.L. Osborne, W.T.S. Huck, Polymer brushes via surface-initiated polymerizations, Chem. Soc. Rev. 33 (1) (2004) 14–22, https://doi.org/10.1039/B210143M.

[22] Y.L. Khung, D. Narducci, Surface modification strategies on mesoporous silica nanoparticles for anti-biofouling zwitterionic film grafting, Adv. Colloid Interface Sci. 226 (2015) 166–186, https://doi.org/10.1016/j.cis.2015.10.009.

[23] Q. Zhou, W. Luo, X. Zhang, Ingenious route for ultraviolet-induced graft polymerization achieved on inorganic particle: Fabricating magnetic poly(acrylic acid) densely grafted nanocomposites for Cu2+ removal, Appl. Surf. Sci. 413 (2017) 181–190, https://doi.org/10.1016/j.apsusc.2017.04.033.

[24] G. Huang, Z. Xiong, H. Qin, J. Zhu, Z. Sun, Y. Zhang, X. Peng, J. ou, H. Zou, Synthesis of zwitterionic polymer brushes hybrid silica nanoparticles via controlled polymerization for highly efficient enrichment of glycopeptides, Anal. Chim. Acta 809 (2014) 61–68, https://doi.org/10.1016/j.aca.2013.11.049.

[25] J.-S. Wang, K. Matyjaszewski, Controlled/“ living” radical polymerization. atom transfer radical polymerization in the presence of transition-metal complexes, J. Am. Chem. Soc. 117 (20) (1995) 5614–5615.

[26] M. Kato, M. Kamigaito, M. Sawamoto, T. Higashimura, Polymerization of methyl methacrylate with the carbon tetrachloride/dichlorotris-(triphenylphosphine) ruthenium (II)/methylaluminum bis (2, 6-di-tert-butylphenoxide) initiating system: possibility of living radical polymerization, Macromolecules 28 (5) (1995) 1721–1723.

[27] C. Huang, T. Tassone, K. Woodberry, D. Sunday, D.L. Green, Impact of ATRP initiator spacer length on grafting poly (methyl methacrylate) from silica nanoparticles, Langmuir 25 (23) (2009) 13351–13360.

[28] L. Zhou, W. Yuan, J. Yuan, X. Hong, Preparation of double-responsive SiO2-g-PDMAEMA nanoparticles via ATRP, Mater. Lett. 62 (8) (2008) 1372–1375, https://doi.org/10.1016/j.matlet.2007.08.057.

[29] M.L. Vera, A. Cánneva, C. Huck-Iriart, F.G. Requejo, M.C. Gonzalez, M. L. Dell’Arciprete, A. Calvo, Fluorescent silica nanoparticles with chemically reactive surface: Controlling spatial distribution in one-step synthesis, J. Colloid Interface Sci. 496 (2017) 456–464, https://doi.org/10.1016/j.jcis.2017.02.040.

[30] M. Ranka, P. Brown, T.A. Hatton, Responsive stabilization of nanoparticles for extreme salinity and high-temperature reservoir applications, ACS Appl. Mater. Interfaces 7 (35) (2015) 19651–19658, https://doi.org/10.1021/acsami.5b04200.

[31] A.R. Khokhlov, E.Y. Kramarenko, Polyelectrolyte/Ionomer behavior in polymer gel collapse, Macromol. Theory Simul. 3 (1) (1994) 45–59, https://doi.org/10.1002/mats.1994.040030104.

[32] N. Cheng, A.A. Brown, O. Azzaroni, W.T.S. Huck, Thickness-dependent properties of polyzwitterionic brushes, Macromolecules 41 (17) (2008) 6317–6321, https://doi.org/10.1021/ma800625y.

[33] V.B. Damodaran, C.J. Fee, T. Ruckh, K.C. Popat, Conformational studies of covalently grafted poly(ethylene glycol) on modified solid matrices using X-ray photoelectron spectroscopy, Langmuir 26 (10) (2010) 7299–7306, https://doi.org/10.1021/la9041502.

[34] S. Chen, S. Chen, S. Jiang, M. Xiong, J. Luo, J. Tang, Z. Ge, Environmentally friendly antibacterial cotton textiles finished with siloxane sulfopropylbetaine, ACS Appl. Mater. Interfaces 3 (4) (2011) 1154–1162.

[35] E. Wikberg, J.J. Verhage, C. Viklund, K. Irgum, Grafting of silica with sulfobetaine polymers via aqueous reversible addition fragmentation chain transfer polymerization and its use as a stationary phase in HILIC, J. Sep. Sci. 32 (12) (2009) 2008–2016, https://doi.org/10.1002/jssc.200800554.

[36] N. Encinas, M. Angulo, C. Astorga, M. Colilla, I. Izquierdo-Barba, M. Vallet-Regí, Mixed-charge pseudo-zwitterionic mesoporous silica nanoparticles with low-fouling and reduced cell uptake properties, Acta Biomater. 84 (2019) 317–327.

[37] R. Khaledialidusti, J. Kleppe, S. Enayatpour, Evaluation and Comparison of Available Tracer Methods for Determining Residual Oil Saturation and Developing an Innovative Single Well Tracer Technique: Dual Salinity Tracer, International Petroleum Technology Conference, 2014.

[38] V. Goulart Isoppo, E. Sangiogo Gil, P.F.B. Gonçalves, F.S. Rodembusch, A. Venturini Moro, Highly fluorescent lipophilic 2,1,3-benzothiadiazole fluorophores as optical sensors for tagging material and gasoline adulteration with ethanol, Sens. Actuators B: Chem. 309 (2020), 127701, https://doi.org/10.1016/j.snb.2020.127701.